

# *Methacrylated chitosan as a polymer with enhanced mucoadhesive properties for transmucosal drug delivery*

Article

Accepted Version

Creative Commons: Attribution-Noncommercial-No Derivative Works 4.0

Kolawole, O. M., Lau, W. M. and Khutoryanskiy, V. V. ORCID: <https://orcid.org/0000-0002-7221-2630> (2018) Methacrylated chitosan as a polymer with enhanced mucoadhesive properties for transmucosal drug delivery. International Journal of Pharmaceutics, 550 (1-2). pp. 123-129. ISSN 0378-5173 doi: 10.1016/j.ijpharm.2018.08.034 Available at <https://centaur.reading.ac.uk/78982/>

It is advisable to refer to the publisher's version if you intend to cite from the work. See [Guidance on citing](#).

Published version at: <https://www.sciencedirect.com/science/article/pii/S0378517318306124>

To link to this article DOI: <http://dx.doi.org/10.1016/j.ijpharm.2018.08.034>

Publisher: Elsevier

All outputs in CentAUR are protected by Intellectual Property Rights law, including copyright law. Copyright and IPR is retained by the creators or other copyright holders. Terms and conditions for use of this material are defined in the [End User Agreement](#).

[www.reading.ac.uk/centaur](http://www.reading.ac.uk/centaur)

**CentAUR**

Central Archive at the University of Reading

Reading's research outputs online

# **Methacrylated chitosan as a polymer with enhanced mucoadhesive properties for transmucosal drug delivery**

Oluwadamilola M. Kolawole<sup>a</sup>, Wing Man Lau<sup>b</sup>, Vitaliy V. Khutoryanskiy<sup>a\*</sup>

<sup>a</sup>Reading School of Pharmacy, University of Reading, Whiteknights, PO Box 224, Reading, RG6 6AD, Berkshire, United Kingdom

<sup>b</sup>School of Pharmacy, The Faculty of Medical Sciences, Newcastle University, Newcastle Upon Tyne, NE1 7RU, United Kingdom

\*Corresponding author at: Reading School of Pharmacy, University of Reading, Whiteknights, PO box 224, Reading, RG6 6AD, United Kingdom. Tel.: +44 (0) 118 378 6119. E-mail address: v.khutoryanskiy@reading.ac.uk

## **Abstract**

Chitosan is a cationic polysaccharide that exhibits mucoadhesive properties which allow it to adhere to mucosal tissues. In this work, we explored chemical modification of chitosan through its reaction with methacrylic anhydride to synthesise methacrylated derivative with the aim to improve its mucoadhesive properties. The reaction products were characterised using <sup>1</sup>H NMR, FTIR and UV-Vis spectroscopy. <sup>1</sup>H NMR and ninhydrin test were used to quantify the degree of methacrylation of chitosan. Turbidimetric analysis of the effect of pH on aqueous solubility of the polymers revealed that the highly methacrylated derivative remained turbid and its turbidity did not change from pH 3 to 9. However, solutions of native chitosan and its derivative with low methacrylation remained transparent at pH 6.5 and exhibited a rapid increase in turbidity at pH > 6.5. The mucoadhesive properties of chitosan and its methacrylated derivatives were evaluated using flow-through method combined with fluorescent microscopy with fluorescein sodium as a model drug. The retention of these polymers was evaluated on porcine bladder mucosa in vitro. The methacrylated derivatives exhibited greater ability to retain fluorescein sodium on the bladder mucosa compared to the parent chitosan. Toxicological studies using MTT assay with UMUC3 bladder cells show no significant differences in toxicity between chitosan and its methacrylated derivatives suggesting good biocompatibility of these novel mucoadhesive polymers.

**Keywords:** Chitosan; Mucoadhesive; methacrylic anhydride; Intravesical drug delivery; UMUC3 cell; toxicity; Wash-out<sub>50</sub>

## 1. Introduction

Ability of water-soluble polymers to adhere to mucosal surfaces, defined as mucoadhesion, has been exploited in the design of mucoadhesive drug delivery systems in the last decades. Various studies have reported the use of mucoadhesive polymers to improve drug delivery in the eye, the nasal cavity, the mouth, the vagina and the urinary bladder (Ludwig 2005; Andrews et al. 2009; Bernkop-Schnürch & Dünnhaupt 2012; Casettari & Illum 2014; Khutoryanskiy 2014; Sosnik et al. 2014; Kolawole et al. 2017; Morales & Brayden 2017). Advantages of mucoadhesive delivery systems include improved drug bioavailability, non-invasive nature of dosage form administration and ease of their application, and the possibility of targeting specific organs, etc.

Chitosan is a cationic polysaccharide that has been widely used in the design of dosage forms for transmucosal drug delivery due to its non-toxic nature and excellent mucoadhesive properties (Bernkop-Schnürch & Dünnhaupt 2012; Casettari & Illum 2014). Chitosan often exhibits superior mucoadhesive properties compared to many other water-soluble polymers; however, there is still a strong interest to improve its properties through chemical modification (Ways et al., 2018). Various dosage forms were developed using chitosan derivatives such as glycol chitosan, trimethyl chitosan, carboxymethyl chitosans, thiolated chitosans, half-acetylated chitosan, glycol chitosan-catechol, methylpyrrolidinone chitosan, and acrylated chitosan and they have all displayed improved retention on mucosal surfaces, thereby extending the duration of action of loaded therapeutics (Ways et al., 2018).

Over the last few years, acrylate- and maleimide-functionalised materials have been explored for transmucosal drug delivery due to their enhanced mucoadhesiveness compared to their parent polymers (Davidovich-Pinhas and Bianco-Peled, 2011; Tonglairoum et al., 2016; Eshel-Green and Bianco-Peled, 2016; Brannigan and Khutoryanskiy, 2017; Shitrit and Bianco-Peled, 2017; Shtenberg et al., 2017; Kaldybekov et al., 2018; Eliyahu, et al., 2018). This is achieved through the quick formation of covalent bonds between acrylate- or maleimide- groups of a mucoadhesive polymer and thiol-groups present in cysteine-rich domains on mucosal surfaces.

Methacrylate groups are also capable of forming covalent bonds with thiols under physiological conditions, similarly to acrylate groups and maleimide. A few studies exist where methacrylate groups have been conjugated to pharmaceutical materials for drug delivery and tissue engineering. For

example, Yu et al (2007) reported the development of methacrylated chitosan that was subsequently cross-linked by radical polymerisation to prepare biodegradable macroporous scaffolds for cell culture applications. Lin et al. (2013) reported the synthesis of methacrylated gelatin that was then used in mixtures with human endothelial colony-forming cells / mesenchymal stem cells for in vivo injection and transdermal photo-crosslinking. However, to our knowledge, the potential of methacrylated polymers as mucoadhesive materials has not been explored yet.

In this study, we developed methacrylated derivatives by reacting chitosan with methacrylic anhydride and evaluated their physicochemical properties, in vitro adhesion to porcine urinary bladder mucosa and cytotoxicity in UMUC3 bladder cells to establish their suitability as materials for transmucosal delivery.

## 2. Materials and methods

### 2.1. Materials

High molecular weight chitosan (CHI, 370 kDa; deacetylation degree  $70.9 \pm 2.2\%$ ), methacrylic anhydride (MA), ninhydrin, trifluoroacetic acid, citric acid, fluorescein sodium, FITC-Dextran (3-5 kDa), 3-(4,5-dimethylthiazol-2-yl)-2,5-diphenyltetrazolium bromide (MTT), foetal bovine serum (FBS) and UMUC3 malignant urothelial cells (Sigma-Aldrich UK); modified Eagle's medium with Earle salts & non-essential amino acids and trypsin-EDTA (Lonza UK); dialysis membrane with molecular weight cut off 12-14 kDa (Medicell International UK); and most chemical reagents (Fischer Scientific UK) were used as received without further purification. Freshly excised porcine urinary bladders were received from PC Turner Abattoir (Farnborough, Hampshire, UK).

### 2.2. Synthesis of methacrylated chitosan

#### 2.2.1. Synthesis of LMeCHI and HMeCHI

Methacrylated chitosan was synthesised by reacting chitosan with methacrylic anhydride at various molar ratios (Table 1) to generate two types of products using the method developed in-house with slight modification (Sogias et al. 2010).

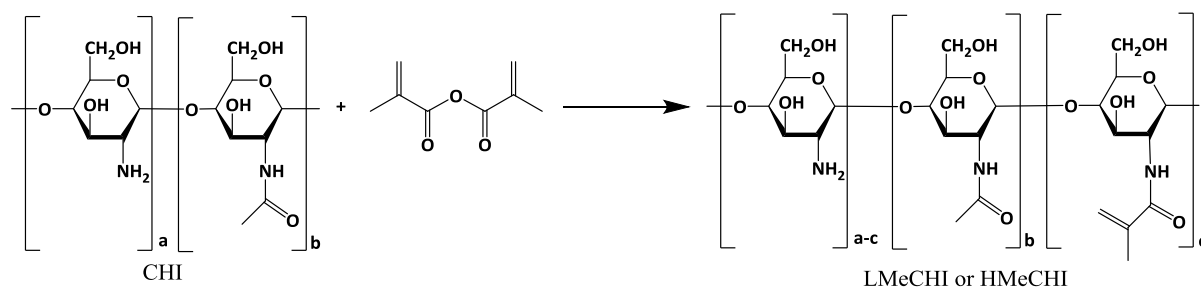


**Fig. 1.** Reaction scheme for the synthesis of methacrylated chitosan: CHI is a parent chitosan and LMeCHI and HMeCHI are chitosans with low and high degrees of methacylation, respectively.

Briefly, 1.5 % w/v chitosan solution (100 mL) was prepared by dissolving predetermined amount of chitosan in 4% v/v acetic acid at 25°C for 12 h. Various amounts of methacrylic anhydride were added slowly to chitosan solution and the mixture was maintained at 40°C, shaken at 60 rpm for 12 h, protected from light. The products were redispersed in deionised water, purified by dialysis (MWCO 12-14 kDa membrane) against 4.5L deionised water with six water changes over 72 h. The final products were freeze-dried using Heto PowerDry LL3000 Freeze Dryer (Thermo Scientific, UK).

**Table 1: Feed ratios for the synthesis of LMeCHI and HMeCHI**

Parameters	LMeCHI	HMeCHI
Concentration, chitosan	1.5 % (w/v)	1.5 % (w/v)
Weight/volume of methacrylic anhydride	1.035g (1 mL)	6.21g (6mL)
Moles of MA per unit mole CHI	0.79	4.65

### 2.3. Characterisation of methacrylated chitosan

#### 2.3.1. <sup>1</sup>H Nuclear magnetic resonance spectroscopy (<sup>1</sup>H NMR)

Solutions of CHI, LMeCHI & HMeCHI (0.6% w/v) were prepared in D<sub>2</sub>O acidified with 30 μL trifluoroacetic acid and allowed to be dissolved overnight at room temperature. The <sup>1</sup>H NMR spectra were recorded using 400 MHz ULTRASHIELD PLUS™ B-ACS 60 spectrometer (Bruker, UK).

### 2.3.2. Fourier Transform-Infrared Spectroscopy (FT-IR)

Solid samples of modified and unmodified chitosan were scanned from 4000 to 400  $\text{cm}^{-1}$ , resolution of 4  $\text{cm}^{-1}$ . Data was processed based on the average of six scans per spectrum generated by the Nicolet iS5-iD5 ATR FT-IR spectrometer (Thermo Scientific, UK).

### 2.3.3. Turbidimetric measurements

The influence of pH on the turbidity of polymer samples was studied according to Sogias et al (2010) with slight modification. Briefly, polymer solutions were prepared in 0.1M acetic acid at room temperature with initial pH 3. NaOH solution (0.1  $\text{mol}\cdot\text{L}^{-1}$ ) was added to increase the pH stepwise and turbidity values of polymer dispersions were measured at 400 nm with Jenway 7315 UV-Vis spectrophotometer (Bibby Scientific, UK).

### 2.3.4. Zeta potential measurements

Zeta potential values of CHI, LMeCHI and HMeCHI solutions/dispersions were determined in folded DTS-1070 capillary cell using Zetasizer Nano-ZS (Malvern Instruments, UK) at 25°C. Solutions/dispersions of chitosan and derivatives (0.4 % w/v) were diluted 1: 20 with ultrapure water prior to analysis. The machine was operated at a refractive index of 1.59 and an absorbance of 0.01. Triplicate readings were recorded with 30 sub-runs per measurement.

### 2.3.5. X-ray Diffractometry

The influence of methacrylation on the crystallinity of chitosan was evaluated using wide-angle powder D8 Advance diffractometer/LYNXEYE XE detector (Bruker, UK). Solid samples of CHI, LMeCHI and HMeCHI were loaded into a capillary tube, sealed with wax to prevent loss and placed onto the goniometer and aligned under a microscope for diffraction analysis, scanning at diffraction ranges from 5 to 50° with a scan step of 0.02°, generating characteristic diffractograms at the rate of 2.5 scans  $\text{min}^{-1}$ .

### 2.3.6. Ninhydrin test to quantify methacrylate groups

The amount of methacrylate groups conjugated to chitosan was quantified using previously published method with slight modification (Shitrit & Bianco-Peled 2017). Briefly, 2 % w/v solution of ninhydrin in DMSO was prepared by stirring for 12 h at room temperature in the dark. Unmodified and modified chitosan solutions (0.05 – 0.5% w/v) were prepared by dissolving in 0.1 M acetic acid, stirred for 18 h in the dark at 25°C. 5mL of ninhydrin solution and 1.25 mL of 4M phosphate buffer (pH 5.4±0.2) were

mixed with 0.5 mL polymer solution. The resultant mixtures were incubated in a water bath at 85°C (OLS 200, Grant, UK) shaken at 60 rpm for 30 min. 1 mL of each mixture was analysed using Jenway 7315 UV-Vis spectrophotometer (Bibby Scientific, UK) at 500 nm.

## 2.4. *Ex vivo* Porcine mucoadhesion studies

### 2.4.5. Preparation of polymer / fluorescein sodium mixture and artificial urine solution

The polymeric solutions/dispersions of CHI, LMeCHI and HMeCHI were prepared by dissolving polymers in 0.1 M acetic acid and stirred overnight. Resultant polymer solutions/dispersions were mixed with 0.1% w/v fluorescein sodium to yield final polymer concentration of 0.4 % w/v (FS/CHI, FS/LMeCHI and FS/HMeCHI, respectively). FITC-dextran 0.4 % (w/v) was dissolved in deionised water overnight under dark conditions at room temperature to serve as negative control.

A protocol developed by Chutipongtanate et al (2010) was used to prepare artificial urine. Briefly, the compounds (Table S1, Supplementary information) were stirred in deionised water for 3 h at room temperature, pH adjusted to 6.2 and made up to a final volume of 2L.

### 2.4.6. Retention on porcine urinary bladder mucosa

Fluorescence microscopy (MZ10F microscope (Leica Microsystems, UK), fitted with an “ET GFP” filter, a Zeiss Imager A1/AxioCam MRm camera; 1296 x 966 pixels; 0.8 x magnification) was used to evaluate the mucosal retention of fluorescein sodium in the presence of the polymeric carriers based on a slightly modified protocol developed in-house (Mun et al. 2016). Freshly excised porcine urinary bladders stored on ice were used in this study within 24 h of procurement. The mucosal side of the bladder tissue was preserved during excision of the required section (about 1.5 x 2.5 cm) and rinsed with artificial urine solution (~ 3 mL) prior to blank tissue imaging. The bladder tissue was placed on a 75 mm x 25 mm glass slide and maintained in an incubator at 37°C during urine wash-out. The following exposure times were used: FITC-dextran (80 ms), FS/CHI (211 ms), FS/LMeCHI and FS/HMeCHI (279 ms). Microscopic images were recorded for each tissue sections before and after applying 100 µL of the polymer sample as well as after each of the five washing cycles with 10 mL artificial urine / cycle at 2 mL/min. The studies were carried out in triplicates. Image J software (National Institute of Health, USA) was used to analyse the microscopic images, generating average fluorescence values as a function of urine volume used for the wash-out. In order to normalise the mean fluorescence values, fluorescence values obtained based on blank tissues were deducted from fluorescence values obtained after each wash-out cycle while the value “1” was used to depict the fluorescence intensity from the tissue prior to wash. From the wash-out trends of the polymers, the



WO<sub>50</sub> values were determined using exponential or polynomial fit of the graphs (Figure S1, Supplementary information), which depicts the volume of artificial urine needed to wash out 50% of the polymer dispersion.

## 2.5. Cell culture and viability experiment

Human urothelial carcinoma cell line, UMUC3 cells (Sigma-Aldrich, UK), were cultured in MEM supplemented with 10% FBS. The cells were cultured in an incubator maintained at 37°C containing 5% CO<sub>2</sub> atmosphere. MTT assay was used to evaluate cell viability with previously reported method with slight modification (Lau et al. 2011). Briefly, UMUC3 cells were seeded in 96-well plate at a density of  $1 \times 10^4$  cells/well. After 24 hours, the cells were treated with polymer solution in growth medium ( $6.25 - 200 \mu\text{g mL}^{-1}$ ) for 4 h. The cells were allowed to grow for further 72 hours. After incubation period, 20  $\mu\text{L}$  of MTT solution ( $5 \text{ mg mL}^{-1}$ ) was added to each well. After 4 h, the supernatant was removed and 100  $\mu\text{L}$  DMSO was added where absorbance was read using the microplate reader (Benchmark-BIO-RAD) at 570 nm. Untreated cells were used as positive control and culture medium was used as background control. Each concentration had three replicates in each experiment and all experiments were done in triplicate. The cell viability was evaluated as a function of viable cells post treatment and total untreated cells. The polymer concentration that yields half-maximum inhibitory response (IC<sub>50</sub> value) was determined based on the best linear fit of the cell viability versus polymer concentration graph.

## 2.6. Statistical analysis

All experimental data were collected in triplicates and data expressed as average  $\pm$  standard deviation. Data were compared using a one-way ANOVA with post-Bonferroni test using GraphPad Prism 5.04 (GraphPad Software Inc., San Diego, California), with  $p < 0.05$  depicting significant difference between data sets.

## 3. Results and discussion

Over the last decade, chitosan has been progressively explored for mucosal delivery of drugs and biotherapeutics due to its biocompatibility, biodegradability, mucoadhesiveness and cell permeation enhancing features (Jayakumar et al. 2010). Recently, acrylated chitosan has been shown to have superior intestinal mucoadhesiveness relative to the thiolated analogue (Shitrit & Bianco-Peled 2017).

The aim of this study was to synthesise methacrylated chitosan using an efficient single step chemical modification. Two types of methacrylated chitosan derivatives with different degrees of substitution

were synthesised and evaluated on their solubility at various pH, mucoadhesiveness and biocompatibility. These derivatives were prepared by the reaction of chitosan with methacrylic anhydride.

### 3.3. Methacrylated chitosan derivatives synthesis

The two methacrylated chitosan derivatives LMeCHI and HMeCHI were synthesised with a yield of 62 % and 24 %, respectively (Table 2). There was no significant difference in their appearance being both off-white colour in nature.

Table 2. Synthetic yield, physical properties and degree of methacrylation (using  $^1\text{H}$  NMR spectroscopy and ninhydrin test) of LMeCHI and HMeCHI

Parameter		LMeCHI	HMeCHI
<b>Synthetic yield</b>		62% (w/w)	24 % (w/w)
<b>Physical appearance</b>		off-white solid	off-white solid
<b>Degree of Methacrylation</b>	$^1\text{H}$ NMR	$11.2 \pm 3.4 \%$	$38.5 \pm 3.9 \%$
	Ninhydrin	$34.3 \pm 2.0 \%$	$55.4 \pm 1.0\%$
	test		

The  $^1\text{H}$  NMR spectra (Figure 2) show the distinctive peaks for chitosan at  $\delta$  2.0 ppm ( $-\text{CH}_3$  from acetylated part of chitosan) as well as 3.09 - 3.8 ppm representing protons from the glucosamine ring. With the methacrylated derivatives, additional peaks are evident at 5.6 and 6.2 ppm depicting the alkenyl double bond from the methacrylate moiety conjugated to chitosan. Also the additional peak at 1.84 ppm appeared in the spectra of methacrylated chitosan is due to  $\text{CH}_3$ - of methacrylic groups. These spectral data are in good agreement with the report by Yu et al. (2007).

The ratio of mean intensity of the proton peaks of the methacrylate groups ( $\delta = 5.6 - 6.2$  ppm) relative to that of the chitosan glucosamine protons ( $\delta = 3.0 - 3.8$  ppm) provides their extent of methacrylation:

$$\text{Methacrylation (\%)} = \frac{\text{Integral of methacrylate protons at 5.6 \& 6.2 ppm} / 2}{\text{Integral of H2-H6 protons} / 6} \cdot 100\% \quad (1)$$

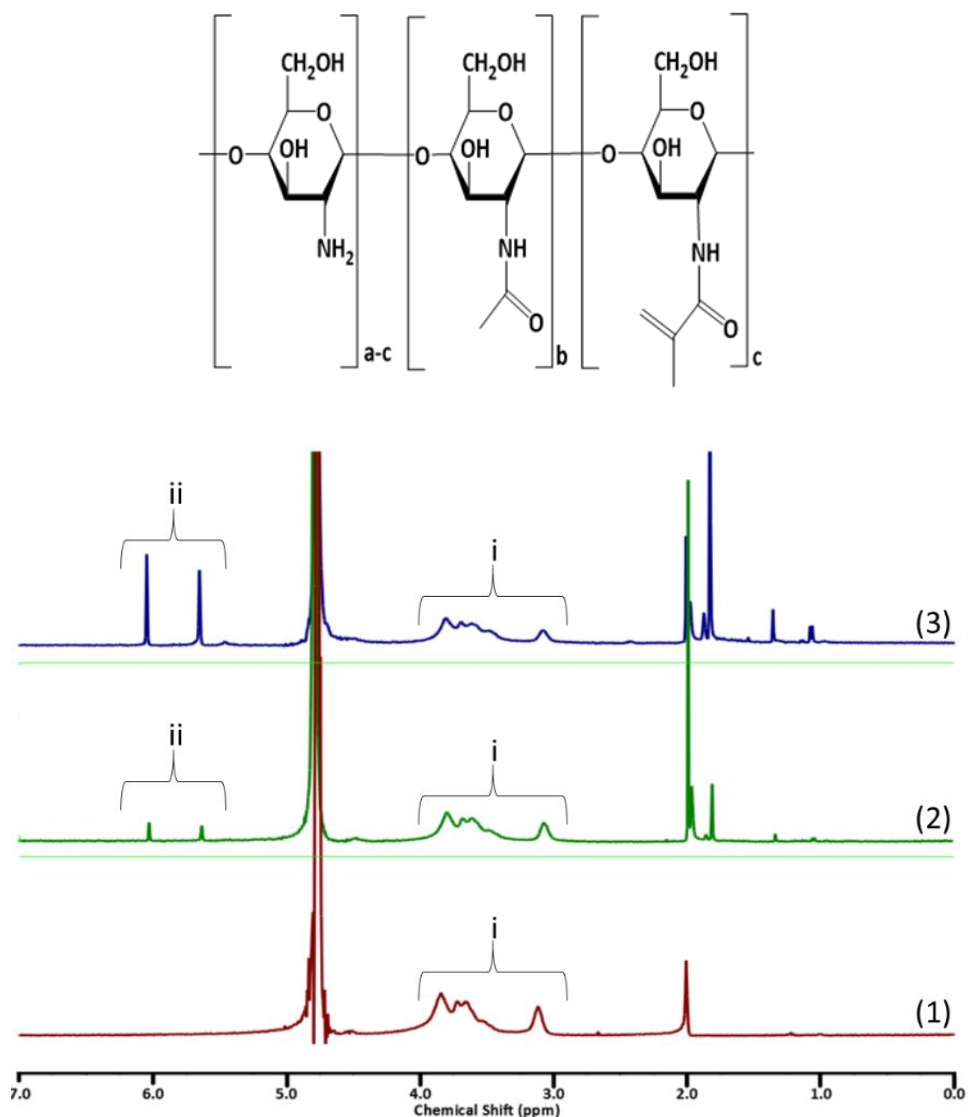


**Fig. 2.** <sup>1</sup>H NMR spectra of CHI (1), LMeCHI (2) and HMeCHI (3) recorded in D<sub>2</sub>O acidified with 1% trifluoroacetic acid. H2-H6 protons of CHI were detected at 3.0-3.8 ppm (i) and vinyl groups of methacrylate segment evident around 5.6-6.2 ppm (ii).

FT-IR shows characteristic absorption bands for chitosan (Fig. 3) at 1026-1151 cm<sup>-1</sup> (amine C-N stretch). Since both chitosan and methacrylate groups display alkyl C-H stretch (2850 and 2930 cm<sup>-1</sup>), the increase in the intensity of the absorption bands is evident of the methacrylated products. The appearance of a new double bond signal at 1537-1653 cm<sup>-1</sup> depicted alkenyl C=C stretch, while amide C=O stretch evident at 1635 cm<sup>-1</sup> in LMeCHI and HMeCHI confirms the methacrylation of chitosan. The FT-IR spectrum of LMeCHI is similar to that of HMeCHI, but differs in terms of the intensity, which is related to their extent of methacrylation.

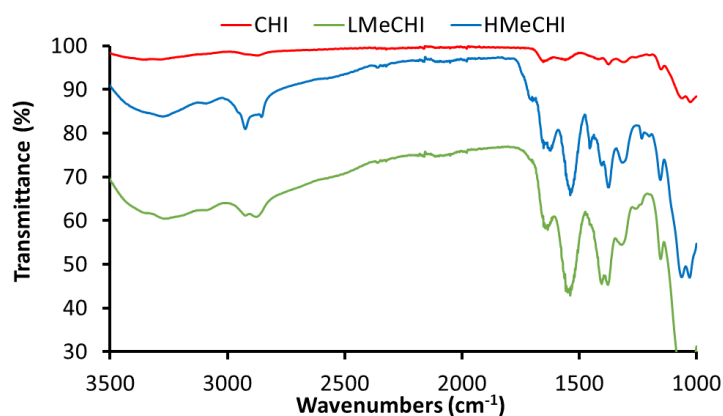


**Fig.3.** FT-IR spectra of CHI , HMeCHI and LMeCHI with characteristic peak at 1537-1635  $\text{cm}^{-1}$  as well as 1653  $\text{cm}^{-1}$  for LMeCHI and HMeCHI depicting alkenyl C=C and amide C=O linkage between chitosan and methacrylate groups, respectively.

### 3.4. Turbidimetric measurements

The effects of pH on turbidity of polymers were analysed where unmodified chitosan shows a turbidity-pH profile (Figure 4) in good agreement with our previous report (Sogias et al, 2010): the solution remains transparent until the pH reaches 6.5; then a further increase in solution pH results in a dramatic increase in turbidity. LMeCHI sample exhibits a pH-dependent solubility similar to unmodified chitosan, with a sharp increase in turbidity observed at  $\text{pH} > 6.5$ . On the other hand, the turbidity profile of HMeCHI is distinctly different, where a slightly turbid colloidal solution was formed at first and maintained in the studied pH range. This is likely to be due to the relatively hydrophobic nature of methacrylate groups that cause aggregation of chitosan macromolecules and formation of micellar structures. The solution of LMeCHI did not show any signs of turbidity at  $\text{pH} < 6.5$  possibly because its degree of methacrylation did not reach a certain threshold to become sufficiently hydrophobic to undergo aggregation. The relatively unchanged turbidity possibly relates to the disruption of semi-crystalline nature of chitosan caused by introduction of bulky methacrylate groups; similar effect was reported for half-acetylated chitosan (Sogias et al, 2010).

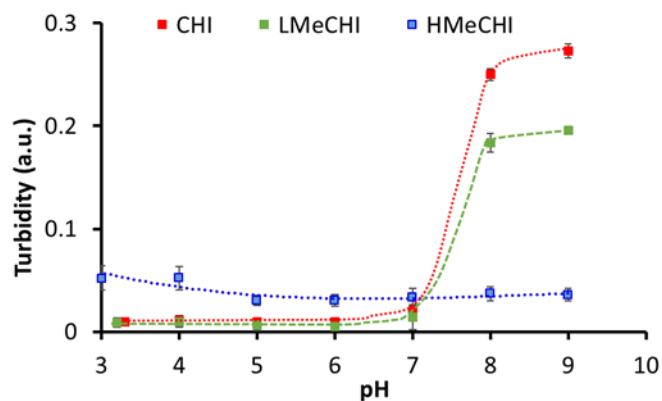


**Fig.4.** Effect of pH on solution turbidity of unmodified chitosan, LMeCHI and HMeCHI. Lines are used as guide to eye.

### 3.5. X-ray Diffractometry

The X-ray diffractogram (Figure 5) shows the unmodified chitosan exhibited two major peaks at diffraction angles ( $2\theta$ ) of  $10.1^\circ$  and  $20.8^\circ$ , which correlate with the peaks displayed by chitosan reported in our earlier publications (Yin et al. 2006; Luo et al. 2008; Sogias et al. 2010). X-ray diffractograms of LMeCHI and HMeCHI (Fig. 4) reveal a decrease in crystallinity upon methacrylation of chitosan with disappearance of the peak at  $8.3^\circ$  and broadening of the peak at  $22.4^\circ$ . This suggests that chitosan has been successfully modified and the modification reduced the ability of chitosan macromolecules to form crystalline domains. This is in good agreement with our previous report on reduction of chitosan's crystallinity upon its re-acetylation (Sogias et al. 2010).

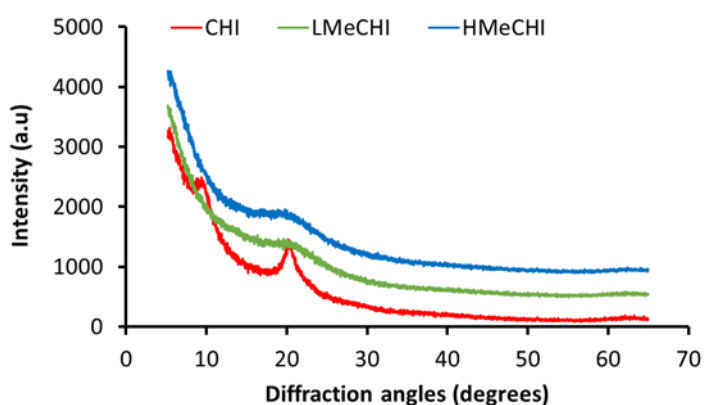


**Fig. 5.** X-ray diffractograms of CHI, LMeCHI and HMeCHI generated at  $2.5 \text{ scans} \cdot \text{min}^{-1}$ , scan angle  $5\text{--}65^\circ$ , scan step size of  $0.02^\circ$ , spectra offset for improved clarity.

### 3.6. Quantification of acrylate groups

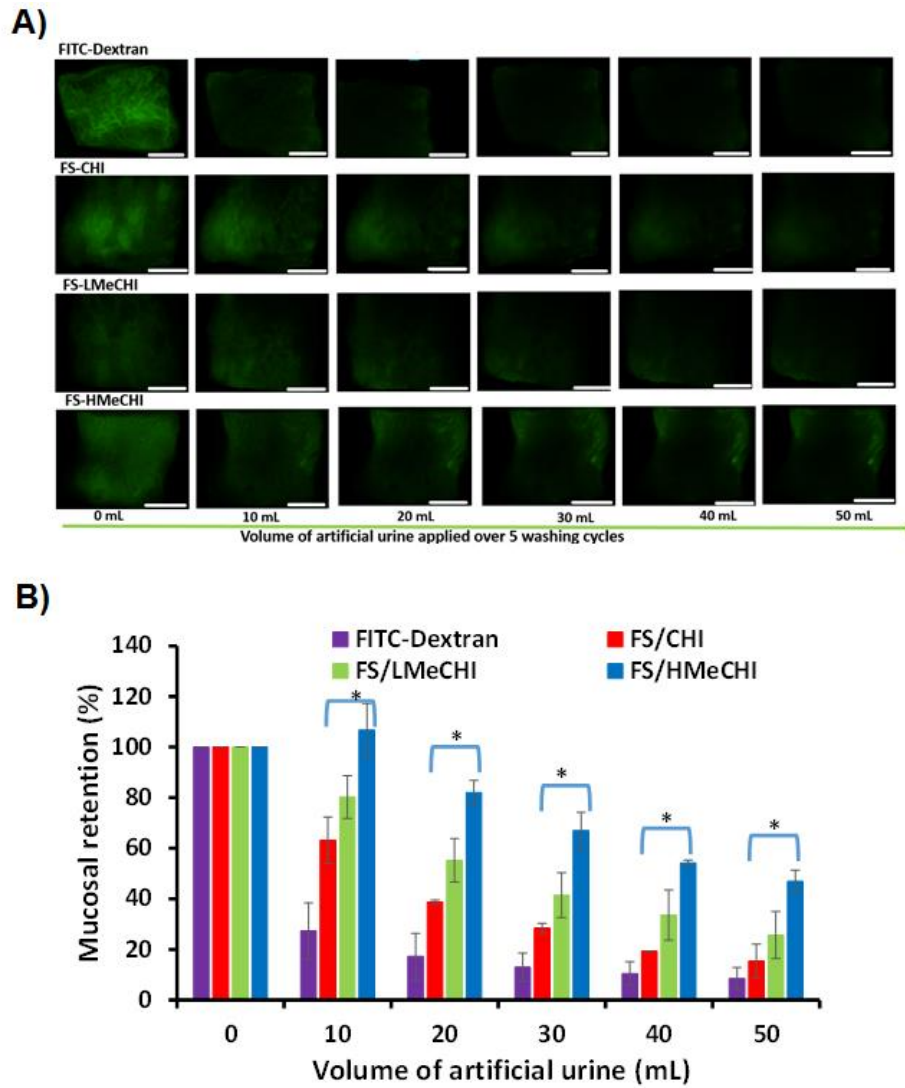
In addition to  $^1\text{H}$  NMR, the ninhydrin test was also used to confirm the degree of methacrylation, where ninhydrin reacts with the unmodified amine groups of chitosan to form a coloured product detectable by UV (Gohel et al. 2006). The slope of the adsorption versus concentration curve of unconjugated chitosan is represented as  $\alpha_{\text{CHI}}$ , while that of LMeCHI and HMeCHI are denoted as  $\alpha_{\text{MeCHI}}$ . Methacrylation percentage can be defined as  $(1 - \alpha_{\text{MeCHI}} / \alpha_{\text{CHI}}) * 100 \%$  (Shitrit & Bianco-Peled 2017).

Table 2 provided data on the extent of methacrylation for LMeCHI and HMeCHI. The degrees of methacrylation for LMeCHI and HMeCHI, calculated from the ninhydrin test (34.3% vs. 55.4%, respectively), were greater than the values calculated using  $^1\text{H}$  NMR spectra (11.2% vs. 38.5%). This may be due to the differences in experimental design as the  $^1\text{H}$  NMR spectra of polymers were recorded in  $\text{D}_2\text{O}$ , acidified with 1 % trifluoroacetic acid, whereas analysis with ninhydrin was performed with the samples dissolved in 0.1 M acetic acid. Different solvents used in these methods could affect the conformation of polymers and availability of functional groups. Potentially,  $^1\text{H}$  NMR technique could underestimate the degree of methacrylation because methacrylate groups could not be on the surface. Nevertheless, the data from both techniques reveal that HMeCHI had a greater degree of methacrylation than LMeCHI.

### 3.7. Mucoadhesion studies

In order to evaluate the mucosal retention, fluorescein sodium was added to the unmodified and methacrylated chitosan solutions prior to the experiment. In the study, the unmodified chitosan, cationic in nature with proven mucoadhesive potential (Sogias et al. 2008), was chosen as the positive control, while dextran with limited mucoadhesiveness (Štorha et al. 2013) served as the negative control.

The mucosal retention of CHI, LMeCHI and HMeCHI on ex vivo bladder tissue was quantified using numerical  $\text{WO}_{50}$  values (Mun et al. 2016).  $\text{WO}_{50}$  is defined as the volume of artificial urine required to remove 50 % of fluorescein sodium from the bladder mucosal surface.



**Fig. 6 (a)** Exemplar microphotographs showing FITC-Dextran, FS/CHI, FS/LMeCHI, and FS/HMeCHI wash-out from porcine urinary bladder with artificial urine solution over 5 washing cycles, scale bar is 2 mm; **(b)** Mucosal retention of fluorescein sodium (FS) from CHI, LMeCHI and HMeCHI on porcine urinary bladder tissue; FITC dextran served as negative control and FS/CHI (unmodified chitosan) as positive control. Result presented as mean  $\pm$  standard deviation,  $n = 3$ , \*depicts significant statistical differences between samples ( $p < 0.05$ ).

WO<sub>50</sub> values for FS/CHI, FS/LMeCHI and FS/HMeCHI were 15 mL, 24 mL and 48 mL, respectively, suggesting that increased methacrylation confers greater mucoadhesive potential on chitosan. FITC-dextran, serving as the negative control was the least retained on the porcine bladder mucosa, displays WO<sub>50</sub> of 7 mL based on extrapolation as 10 mL of artificial urine was used for each wash-out cycle (Fig. 6) similar to that reported previously (Mun et al. 2016). The superior mucoadhesive

behaviour of HMeCHI as shown in Fig. 6 is likely due to the presence of higher percentage of unsaturated methacrylate groups that formed covalent bonds with thiols of mucin present on the mucosal surface (Shitrit & Bianco-Peled 2017).

The zeta potential of  $13.3 \pm 3.2$ ,  $41.4 \pm 7.0$  and  $54.4 \pm 1.9$  mV were recorded for 0.02% w/v polymer solutions/dispersions of CHI, LMeCHI and HMeCHI, respectively. The degree of positive charge of these polymers supports their favourable interaction with the negatively charged mucosal surface (Khutoryanskiy, 2014). Moreover, the methacrylated chitosan may also facilitate loosening of tight junctions between cells which promotes cellular internalisation of the drug carrier (Smith et al. 2004). There was statistical difference in the mucoadhesive profile of parent chitosan and the highly methacrylated derivative (HMeCHI) after five washing cycles ( $p < 0.05$ ).

Interestingly, HMeCHI displayed a similar  $WO_{50}$  value (48 mL) to PEGylated maleimide functionalised liposomes ( $WO_{50}$  value 48 mL) evaluated for bladder delivery (Kaldybekov et al. 2018), suggesting that functionalisation of chitosan with methacrylate moieties may facilitate comparable covalent interactions with mucosal glycoproteins, achievable with maleimide derivatisation of liposomes.

### 3.8. Cell viability studies

Distressing symptoms like painful sensation during urination are common in bladder cancer. So, drug carriers intended for bladder cancer therapy should not aggravate the discomfort experienced by patients. UMUC3 human bladder carcinoma cells have been used as *in vitro* model for studying the cytotoxic and irritation effect of drug delivery systems intended for bladder cancer treatment (Zhang et al. 2014; Lu et al. 2015; Lu et al. 2016). The selected duration of cell incubation with polymer solution (4 h) was clinically relevant as most drug carriers required such contact time with diseased tissues for effective therapy (Mugabe et al. 2011). The safety of methacrylated gellan gum has been previously reported (Coutinho et al. 2010), but there was no data available for methacrylated chitosan.



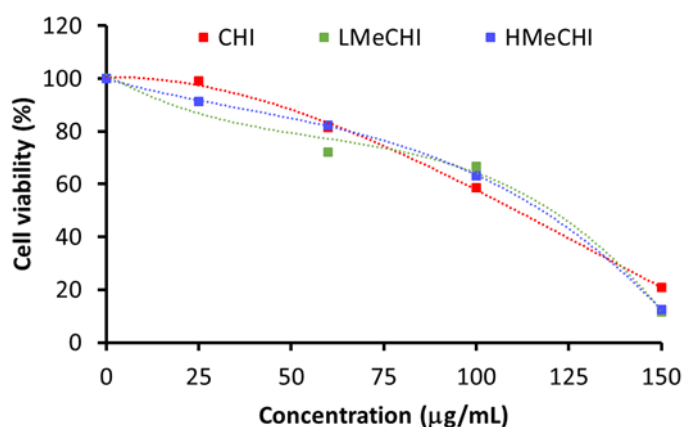


**Fig.7.** UMUC3 cell viability studies using CHI, LMeCHI and HMeCHI. Polymer treatment for 4 h and cell viability studied at 72 h post exposure to polymers. The untreated cells served as the control. Cell viability is normalised against the control; n=3. Lines are used as guide to eye. Error bars are not shown on this figure to avoid overcrowding.

The UMUC3 cell growth inhibitory effect of the polymers was studied over 72 h (Fig. 7). CHI, LMeCHI and HMeCHI displayed  $IC_{50}$  values of  $108.40 \pm 5.81$ ,  $96.17 \pm 5.27$  and  $104.16 \pm 4.81 \mu\text{g mL}^{-1}$ , respectively. One-way ANOVA statistical analysis shows that there is no statistically significant differences in the  $IC_{50}$  values between all three polymers ( $p > 0.05$ ). This suggests the methacrylated chitosan is as safe as the unmodified chitosan and thus could be exploited further for intravesical drug delivery due to its superior mucoadhesive features.

## 4. Conclusion

To our knowledge, this is the first report where the pH-dependent solubility, mucoadhesive properties and safety profile of unmodified and methacrylated chitosan have been compared. Methacrylate groups were grafted onto chitosan through the reaction of its amino-groups with methacrylic anhydride in order to synthesise novel mucoadhesive polymers. The volume ratio of high molecular weight chitosan to methacrylic anhydride was varied to generate two types of methacrylated chitosan that differed in terms of their degree of methacrylation.  $^1\text{H}$  NMR and ninhydrin test analysis confirmed the successful synthesis of the methacrylated products.

Methacrylation of chitosan has been identified as a simple and viable synthetic strategy to generate drug carriers with greater mucoadhesive properties. This novel drug carrier can be used to formulate

dosage forms that allows prolonging drug residence time in the bladder thereby improving extent of drug absorption thus therapeutic outcomes for bladder cancer treatment. Methacrylated chitosan with enhanced mucoadhesive properties could also be of interest for application in other areas of transmucosal drug delivery. Future research using these mucoadhesive chitosan derivatives may include preparation of formulations with various active pharmaceutical ingredients, studies of their physicochemical characteristics and drug release studies.

## Acknowledgements

The Chemical Analysis Facility (University of Reading) is acknowledged for providing access to FTIR and  $^1\text{H}$  NMR spectroscopies as well as to x-ray diffraction. The authors are grateful to Mr. Nicholas Spencer for his help with X-ray diffraction analysis, and to Dr Brett Symonds for analysis of chitosan samples by gel permeation chromatography. The University of Reading, the Leche Trust and Gilchrist Educational Trust provided financial assistance supporting postgraduate studies of OMK.

## References

- Andrews, G.P., Lavery, T.P. & Jones, D.S., 2009. Mucoadhesive polymeric platforms for controlled drug delivery. *European Journal of Pharmaceutics and Biopharmaceutics*, 71(3), pp.505–518.
- Bernkop-Schnürch, A. & Dünnhaupt, S., 2012. Chitosan-based drug delivery systems. *European Journal of Pharmaceutics and Biopharmaceutics*, 81(3), pp.463–469.
- Brannigan, R.P. & Khutoryanskiy, V. V., 2017. Synthesis and evaluation of mucoadhesive acryloyl-quaternized PDMAEMA nanogels for ocular drug delivery. *Colloids and Surfaces B: Biointerfaces*, 155, pp.538–543.
- Casettari, L. & Illum, L., 2014. Chitosan in nasal delivery systems for therapeutic drugs. *Journal of Controlled Release*, 190, pp.189–200. Available at: <http://dx.doi.org/10.1016/j.jconrel.2014.05.003>.
- Chutipongtanate, S. & Thongboonkerd, V., 2010. Systematic comparisons of artificial urine formulas for in vitro cellular study. *Analytical biochemistry*, 402(1), pp.110–2.
- Coutinho, D.F. et al., 2010. Modified Gellan Gum hydrogels with tunable physical and mechanical properties. *Biomaterials*, 31(29), pp.7494–7502.
- Davidovich-Pinhas, M. & Bianco-Peled, H., 2011. Alginate-PEGAc: A new mucoadhesive polymer. *Acta*

- Biomaterialia*, 7(2), pp.625–633.
- Eliyahu, S., Aharon, A., Bianco-Peled, H., 2018. Acrylated chitosan nanoparticles with enhanced mucoadhesion. *Polymers*, 10(2), p.106.
- Eshel-Green, T. & Bianco-Peled, H., 2016. Mucoadhesive acrylated block copolymers micelles for the delivery of hydrophobic drugs. *Colloids and Surfaces B: Biointerfaces*, 139, pp.42–51.
- Gohel, V. et al., 2006. Quantitative determination of chitosans by ninhydrin. *Carbohydrate Polymers*, 38(2), pp.255–257.
- Jayakumar, R. et al., 2010. Biomedical applications of chitin and chitosan based nanomaterials - A short review. *Carbohydrate Polymers*, 82(2), pp.227–232.
- Kaldybekov, D.B. et al., 2018. Mucoadhesive maleimide-functionalised liposomes for drug delivery to urinary bladder. *European Journal of Pharmaceutical Sciences*, 111, pp.83–90.
- Khutoryanskiy, V. V., 2014. *Mucoadhesive Materials and Drug Delivery Systems*, John Wiley & Sons.
- Kolawole, O.M. et al., 2017. Advances in intravesical drug delivery systems to treat bladder cancer. *International Journal of Pharmaceutics*, 532(1), pp.105–117.
- Lau, W.M. et al., 2011. Therapeutic and cytotoxic effects of the novel antipsoriasis codrug, naproxyl-dithranol, on HaCaT cells. *Molecular Pharmaceutics*, 8(6), pp.2398–2407.
- Lin, R.Z. et al., 2013. Transdermal regulation of vascular network bioengineering using a photopolymerizable methacrylated gelatin hydrogel. *Biomaterials*, 34(28), pp.6785–6796.
- Lu, S. et al., 2016. Co-delivery of peptide-modified cisplatin and doxorubicin via mucoadhesive nanocapsules for potential synergistic intravesical chemotherapy of non-muscle-invasive bladder cancer. *European Journal of Pharmaceutical Sciences*, 84, pp.103–115.
- Lu, S. et al., 2015. Mucoadhesive polyacrylamide nanogel as a potential hydrophobic drug carrier for intravesical bladder cancer therapy. *European Journal of Pharmaceutical Sciences*, 72, pp.57–68.
- Ludwig, A., 2005. The use of mucoadhesive polymers in ocular drug delivery. *Advanced Drug Delivery Reviews*, 57(11), pp.1595–1639.
- Luo, K. et al., 2008. Mucoadhesive and elastic films based on blends of chitosan and hydroxyethylcellulose. *Macromolecular Bioscience*, 8(2), pp.184–192.

- Morales, J.O. & Brayden, D.J., 2017. Buccal delivery of small molecules and biologics: of mucoadhesive polymers, films, and nanoparticles. *Current Opinion in Pharmacology*, 36, pp.22–28.
- Mugabe, C. et al., 2011. In vivo evaluation of mucoadhesive nanoparticulate docetaxel for intravesical treatment of non-muscle-invasive bladder cancer. *Clinical Cancer Research*, 17(9), pp.2788–2798.
- Mun, E.A., Williams, A.C. & Khutoryanskiy, V. V., 2016. Adhesion of thiolated silica nanoparticles to urinary bladder mucosa: Effects of PEGylation, thiol content and particle size. *International Journal of Pharmaceutics*, 512(1), pp.32–38.
- Shitrit, Y. & Bianco-Peled, H., 2017. Acrylated chitosan for mucoadhesive drug delivery systems. *International Journal of Pharmaceutics*, 517(1–2), pp.247–255.
- Shtenberg, Y. et al., 2017. Alginate modified with maleimide-terminated PEG as drug carriers with enhanced mucoadhesion. *Carbohydrate Polymers*, 175, pp.337–346.
- Smith, J., Wood, E. & Dornish, M., 2004. Effect of chitosan on epithelial cell tight junctions. *Pharmaceutical Research*, 21(1), pp.43–49.
- Sogias, I.A., Khutoryanskiy, V. V. & Williams, A.C., 2010. Exploring the factors affecting the solubility of chitosan in water. *Macromolecular Chemistry and Physics*, 211(4), pp.426–433.
- Sogias, I.A., Williams, A.C. & Khutoryanskiy, V. V., 2008. Why is chitosan mucoadhesive? *Biomacromolecules*, 9(7), pp.1837–1842.
- Sosnik, A., Das Neves, J. & Sarmiento, B., 2014. Mucoadhesive polymers in the design of nano-drug delivery systems for administration by non-parenteral routes: A review. *Progress in Polymer Science*, 39(12), pp.2030–2075.
- Štorha, A., Mun, E. A. & Khutoryanskiy, V. V., 2013. Synthesis of thiolated and acrylated nanoparticles using thiol-ene click chemistry: towards novel mucoadhesive materials for drug delivery. *RSC Advances*, 3(30), p.12275-12279.
- Tonglairoom, P. et al., 2016. Maleimide-bearing nanogels as novel mucoadhesive materials for drug delivery. *J. Mater. Chem. B*, 4(40), pp.6581–6587.
- Ways, T., Lau, W. & Khutoryanskiy, V., 2018. Chitosan and Its Derivatives for Application in Mucoadhesive Drug Delivery Systems. *Polymers*, 10(3), p.267.

- Yin, J. et al., 2006. Miscibility studies of the blends of chitosan with some cellulose ethers. *Carbohydrate Polymers*, 63(2), pp.238–244.
- Yu, L.M.Y., Kazazian, K. & Shoichet, M.S., 2007. Peptide surface modification of methacrylamide chitosan for neural tissue engineering applications. *Journal of Biomedical Materials Research - Part A*, 82(1), pp.243–255.
- Zhang, Q. et al., 2014. Functionalized mesoporous silica nanoparticles with mucoadhesive and sustained drug release properties for potential bladder cancer therapy. *Langmuir*, 30(21), pp.6151–61.